Use of multi-factorial analysis to determine the quality of cellulose nanofibers. Effect of nanofibrillation treatment and residual lignin content

Eduardo Espinosa[a], Fleur Rol[b], Julien Bras[bc], Alejandro Rodríguez[a]

[a] Universidad de Córdoba, Departamento de Ingeniería Química, Campus de Rabanales, 14014 Córdoba, Spain

[b] Univ. Grenoble Alpes, CNRS, Grenoble INP, LGP2, F-38000 Grenoble, France

[c] Institut Universitaire de France (IUF), F-75000 Paris, France

* Corresponding author: eduardo.espinosa@uco.es

Abstract

The aim of this work is to analyze different methods of nanocellulose production from wheat straw and study the effect of the lignin in the nanocellulose quality and on the characteristics of the films produced. Wheat straw was subjected to a soda pulping process to obtain unbleached cellulosic pulp. The cellulosic pulp was bleached with $NaClO_2$ in order to remove the lignin of the fiber. Both bleached and unbleached pulps were used to obtain nanocellulose using mechanical pretreatment (PFI refining) and treatments (high pressure homogenization, twin-screw extruder and ultrafine friction grinder). The effect of the nanofibrillation treatments and the residual lignin content on cellulose nanofibers production was analyzed by means of a deep characterization. A multi-factorial quality index was used to score the cellulose nanofibers produced to enable a benchmarking study between different sources, processes and characteristics. In addition, an energetic study of the production process was carried out for the different treatments. The different nanofibers were used to produce cellulose nanofibers-based films and characterized in order to establish a relationship between the characteristics of cellulose nanofibers and the characteristics of the final product.

Keywords: wheat straw, cellulose nanofibers, nanofibrillation treatments, lignin effect, films properties, quality

1. Introduction

Nanocelluloses are cellulosic elements having nanometric diameters (less than 100 nm) (Wang et al. 2019). Nanocellulose, as cellulose, is a renewable, biodegradable and non-toxic material, in addition, its excellent mechanical and optical properties extends its range of application to different sectors such as food packaging (Espinosa et al. 2019a), papermaking industry (Boufi et al. 2016), construction (Claramunt et al. 2019), biomedicine (Chinga-Carrasco 2018), environmental remediation (Torstensen et al. 2019), electronic and energy (Agate et al. 2018, Du et al. 2017), etc. Three types of nanocelluloses can be distinguished: cellulose nanocrystals (CNC), cellulose nanofibers (CNF) and bacterial nanocellulose (BNC). Although all types of nanocellulose have a similar chemical composition, they are different in morphology, particle size, crystallinity and other properties, depending on the source and extraction methods used. The cellulose nanofibers also known as nanofibrillated cellulose, are a type of flexible, elongated, cross-

linked nanocellulose that can be extracted from cellulose fibers by mechanical treatments. CNF are generally produced by mechanical delamination of cellulose fibers after a pre-treatment that facilitates the fiber disintegration. These pre-treatments avoid the occlusion of the equipment where the disintegration process takes place, and reduce the number of passes or treatment time, with the reduction in energy consumption that this entails. Several fiber pre-treatments have been described such as enzymatic hydrolysis (Pääkkö et al. 2007), partial carboxymethylation (Fall et al. 2011), catalytic oxidation using 2,2,6,6-tegramethylpiperidine-1-oxyl (TEMPO) (Saito et al. 2007) and mechanical refining (Yousefi et al. 2011). After pretreatment, the fiber is subjected to a mechanical disintegration process, including: high pressure homogenization (Li et al. 2012), microfluidization (Wang et al. 2015), friction grinding (Kumode et al. 2017), extrusion (Rol et al. 2017), cryocrushing (Chakraborty, Sain and Kortschot 2005) and high intensity ultrasonication (Chen et al. 2011).

There are several cellulose sources in nature that can be used to produce cellulose nanofibers. Among these sources are wood species such as pinecone (Rambabu et al. 2016), eucalyptus (Campano et al. 2018) and spruce (Rojo et al. 2015), as well as different lignocellulosic residues, which have also been successfully used to produce cellulose nanofibers, such as wheat straw (Espinosa et al. 2017b), sugarcane bagasse (de Campos et al. 2013), olive tree pruning (Fillat et al. 2018), cotton linters (Morais et al. 2013), etc. For each raw material, due to the numerous possible combinations between pre-treatments and existing treatments for CNF production, there is a high variability of CNF that can be produced. Siqueira et al. described that small differences in processing produces large differences in the characteristics of the CNF, existing tens of distinct CNF from the same starting fiber (Siqueira et al. 2010).

This high variability in the final characteristics of the CNF, makes it necessary to develop parameters that allow comparison between different raw material and processes for the optimization of production and choice of the suitability of the final application. Numerous parameters have been used to determine the quality of the CNF produced, such as nanofibrillation yield (also known as nanofibrillated fraction, degree of fibrillation or fibrillation degree) which indicates what proportion of nanofibrillated material is in the CNF suspension (Besbes, Alila and Boufi 2011); the optical transmittance or turbidity as indirect indicators of the nanofibrillation yield due to the light scattering produced by large particles in a suspension; the cationic demand related to the specific surface of the CNF, which makes it possible to know the efficacy of nanofibrillation (Tarrés et al. 2017b); as well as other techniques to determine the size of nanofibers such as electron microscopy (Chinga-Carrasco 2013), dynamic light scattering (Espinosa et al. 2017b) and asymmetric flow field flow fractionation (Ruiz-Palomero, Laura Soriano and Valcárcel 2017). The use of optical methods to determine the quality of CNF has been widely used, but nevertheless has its limitations, as its observation may involve not considering fraction containing macrofibers. In addition, this type of technique involves the use of high-level microscopy tools, which is difficult to incorporate into a production process (Desmaisons et al. 2017). There are many more parameters that allows us to measure the

properties of these CNF such as rheology, crystallinity, mechanical properties, surface chemistry, degree of polymerization, etc.
Although with all these parameters different samples can be differentiated, it can only be ordered qualitatively, not by synthesizing the results and having to be compared test by test.

Desmaisons et al. (2017) proposed a multi-criteria method that enables to obtain a single quantitative grade which allows the monitorization of the production of nanocellulose on an industrial and laboratory scale. In addition, only simple and standard equipment was used making it easy to incorporate into the production process. In this work, two indices were established, a broad index consisting of 8 parameters (both indirect on CNF suspension and indirect on CNF nanopaper), and a simplified index where these 8 parameters were grouped into 4 by means of a principal component analysis (PCA). For each parameter a database was established with literature data, test on commercial CNF suspension and test on CNF suspension obtained in laboratory. Samples used as reference for the database range from poorly fibrillated cellulose to highly nanofibrillated cellulose. The trends and values observed in the database were used to obtain tables of correspondence for each parameter by a single equation allowing the conversion of raw data into a score, associating the value obtained from each parameter with a score out of 10. In this work, the influence of the drying process, the hemicellulose content and pre-refining process on the quality index of the obtained CNF was shown.

Since then, several authors have used this index to study the influence of the characteristics of the pulp and the process in the production of CNF suspension and to establish an optimum value for each application in which it is used. In this work, CNF from wheat straw soda pulp were produced by different mechanical treatments. The abbreviated quality index (QI*) was used to compare the suitability of each treatment in the production of cellulose nanofibers as well as the effect of the residual lignin content on the final properties. On the other hand, the energy demand of each treatment in cellulose nanofibers production was also studied. The different cellulose nanofibers, both, lignin-free (CNF) and lignin-containing (LCNF) were used to produce nanocellulose-based films and their physical, mechanical, barrier and antioxidant properties were analyzed in order to relate the characteristics of the cellulose nanofibers and their application in films.

2. Materials and Methods

2.1. Materials.

Wheat straw provide by an independent farmer was used in this work after a manual screening to remove undesired elements. All of the materials and chemicals were used as received from the producers: acetic acid (CH_3COOH) (ACS reagent, ≥99.7%); acetone (C_3H_6O); hydrochloric acid (HCl); sodium chloride (NaCl) (>99%); sodium hydroxide (NaOH); sodium chlorite ($NaClO_2$) (Sigma Aldrich, technical grade 80%); poly-

DADMAC (BTG 0.01 N); Pes-Na (BTG 0.01 N) and 2,2'-Azino-bis(3-ethylbenzothiazoline-6-sulfonic acid) diammonium salt (Sigma Aldrich, >98%).

2.2. Cellulose Pulp Production

Wheat straw was subjected to a soda pulping process at 100 °C, 150 min, 7% soda (over dry matter), and a liquid/solid ratio of 10:1. The cellulose pulp characteristics was determined using the following standards, beating degree (TAPPI T-227), yield (gravimetric method), α-cellulose (T-9m54), lignin (T-203os61), holocellulose (T-222), ash (T-211), ethanol extractable T-204), Kappa number (T-236cm85) and viscosity (T-30om94).

2.3. Lignocellulose Nanofibers Production

Cellulose nanofibers were obtained for the nanofibrillation of wheat straw cellulosic pulp by three different treatments. Before each treatment, a concentration of 10% of cellulosic fiber was refined, as mechanical pretreatment, using a PFI Beater until getting a Schopper-Riegler degree of 90 according to ISO 5267-1. A fiber suspension at 2 wt % were fibrillated using an ultrafine friction grinder (model MKZA6-2, disk model MKG-C 80, Masuko Sangyo Co., Ltd., Japan) equipped with recirculation at 2500 rpm for 2.5 h. The maximum gap used between the two disks was -10. A suspension adjusted between 18 and 20 wt % was passed through a twin-screw extruder (Model Thermoscientific HAAKE Rheomex OS PTW 16 + HAAKE PolyLab OS RheoDrive 7) with a ratio (L/D) of 45. The temperature was maintained close to 10 °C, and the speed was 400 rpm. A 1.5 wt % fiber suspension was passed through a high pressure homogenizer (PANDA GEA 2 K NIRO) following the next sequence: 4 passes at 300 bars, 3 passes at 600 bars and 3 passes at 900 bars (Espinosa et al. 2019b)

2.4. Lignocellulose Nanofibers Characterization

The different cellulose nanofibers were characterized in terms of yield of nanofibrillation, optical transmittance, carboxyl content and cationic demand. The nanofibrillation yield was performed according to the method proposed by Besbes et al. (2011). The optical transmittance of a 0.1% cellulose nanofiber suspension was measured using a Lambda 25 UV-Spectrometer and used as an indirect indicator of the nanofibrillation yield. The carboxyl content (CC) of the cellulose nanofiber was determined using conductometric titration as described in literature (Besbes et al. 2011). The Cationic Demand of cellulose nanofiber was determined using of a Mütek PCD 05 particle charge detector following the methodology described by Espinosa et al. (2017a). The specific surface area of cellulose nanofiber and the theoretical diameter were calculated considering the stoichiometric relationship of the poly-DADMAC absorption on the hydroxyl and carboxyl groups of the cellulose nanofibers surface (Espinosa et al. 2016). In order to corroborate the theoretical diameter estimation, cellulose nanofibers were dispersed at a 10^{-2} wt % concentration in water, and one drop was deposited on an Icon atomic force microscope with an OTESPA. The intrinsic viscosity (η_s) of the cellulose nanofibers was calculated following the ISO 5351:2010 standard. The intrinsic viscosity (η_s) and the

degree of polymerization were related according to the following equations (Marx-Figini 1987):

DP (< 950): $DP = (\eta_s/0.42)$

DP (> 950): $DP^{0.76} = (\eta_s/2.28)$

The values of degree of polymerization were used to calculate the length of the nanofiber using the following equation (Shinoda et al. 2012):

$$Length\ (nm) = 4.286 \cdot DP - 757$$

All the measurements were made at least in triplicate and the mean value and standard deviation were calculated.

2.5. Energy Demand Calculation

The energy demand calculation for high pressure homogenizer and ultrafine friction grinder was measured using an energy measuring equipment, obtaining the energy consumption of the equipment or, which is the same, the energy required from the electrical grid. The specific mechanical energy (SME) consumed by the TSE was calculated using the following equation (Gogoi, Oswalt and Choudhury 1996; Liang, Huff and Hsieh 2002; Domenech, Peuvrel-Disdier and Vergnes 2013):

$$SME = \frac{N * C * Q}{N_{max} * P_{max} * C_{max}}$$

Where N is the speed in rpm, N_{max} the maximal speed in rpm (1100 rpm), P_{max} the maximal pressure (7 kW), C (N.m) the torque measured on the extruder motor, C_{max} the maximal torque (130 N.m) and Q the dry flow in t/h.

2.6. Simplified quality index (QI*)

The different cellulose nanofibers were evaluated according to the simplified quality index (QI*) reported by Desmaisons et al. (2017). In contrast with the original quality index, the simplified version is based on four parameters (nanosized fraction, turbidity, average size of microparticles and Young's modulus), which are pondered and used for the QI* calculation according to the next equation:

$$QI^* = 0.3P_1 + (-0.03P_2) - 0.071P_3^2 + 2.54P_3 - 5.35 \cdot lnP_4 + 59.90$$

where P_1 is the nanosized fraction (%), P_2 is the turbidity (NTU), P_3 is Young's modulus (GPa) and P_4 is the average microparticle size (μm^2).

2.6.1. Nanosized fraction

The nanosized fraction analysis was performed according to the protocol described by Naderi et al. (2015). A 0.02 wt% cellulose nanofibers suspension was centrifuged at 1000g for 15 min to remove the larges components. The concentrations in the supernatant part was measured after and before centrifugation and used to measure the nanosized fraction using the following equation:

$$NF\ (\%) = \frac{Cac}{Cbc} \cdot 100$$

Where Cac and Cbc correspond to the concentration after and before centrifugation.

2.6.2. Turbidity

The turbidity of a 0.1% wt cellulose nanofibers suspension was measured using a portable turbidimeter (AL 250 T-IT) with a technique range of 0.01 – 1100 NTU. Ten measurement for each suspension was performed and used to obtain an average value.

2.6.3. Young's modulus

For the measurement of the mechanical properties, nanopapers of the different cellulose nanofibers were prepared by filtration of a cellulose nanofiber suspension (2 g of dry weight) through a standard sheet former equipped with a nylon sieve with a mesh of 1 µm. The nanopapers were dried in a dryer at 90 ºC until constant weight and conditioned in a weather chamber 25 ºC and 50% humidity for 48 h according to the requirements of ISO 5269-2. The Young's modulus was obtained using an Instron 5965 machine equipped with a load cell of 5 kN capacity. Samples of 100 mm x 15 mm were prepared at a cross-head speed of 5 mm/min.

2.6.4. Average microparticle size

The average microparticle size was measured by the analysis of optical microscopy mages of a 0.5 wt% concentration of cellulose nanofiber suspension using a Carl Zeiss Axio Imager M1 in transmission mode and equipped with an Axio Cam MRc 5 digital camera. Five images of each samples were taken and analyzed using software ImageJ.

2.7. Cellulose nanofibers-based films characterization

Films of 0.5 g were prepared by the solvent casting technique of a 0.5 wt% cellulose nanofibers suspension. The suspension was prepared with an Ultraturrax Homogenizer for 5 min at 15000 rpm. The properly dispersed suspension was casted in polypropylene petri dishes (ø=9 cm) and dried at room temperature until water evaporation. The mechanical properties (tensile strength, elongation at break and Young's modulus) of the films was determined using an Instron 5965 machine equipped with a load cell of 5 kN capacity in accordance with the standard ASTM D638. Ten test specimens of 65 mm x 15 mm for each sample was prepared and conditioned for 48h at 25 °C and 50% humidity before testing. The surface roughness of the films was analyzed with a Lehmann laser profilometer (Lehmann Mess-Systeme AG Baden-Dätwil, Germany). The acquired topography images, 1 x 1 mm with a resolution of 1 µm/pixel, were processed with the SurfCharJ plugin for ImageJ as described by Chinga-Carrasco et al. (2014). The water vapor permeability (WVP) was determined according to ASTM E96/E96M-10 standard. Films were sealed on plastic containers which were placed in a controlled chamber at 25 °C and a 50% humidity and weighted at different times interval to calculate the mass gain (Karkhanis et al. 2018). The oxygen transmission rate (OTR) was analyzed using a Mocon OX-TRAN® 1/50 test system (Mocon, Minneapolis, MN, USA) at 50% humidity and 23 °C. The antioxidant activity of the films was determined by the ABST assay. A 7 mM

ABTS and 2.45 mM potassium pershulphate was prepared and kept in dark overnight before using. A square of 1 cm^2 of the film was added in 4 mL of the radical solution and de absorbance was measured at 734 nm against ethanol as blank. The antioxidant power of the samples was calculated following the protocol described by García et al. (2012)

3. Results and discussion

3.1. Cellulose nanofibers isolation from wheat straw

In order to facilitate the accessibility of cellulose fibers, wheat straw was subjected to soda pulping process, which is the one that presents the best results to produce cellulosic pulp with optimal characteristics for the isolation of cellulose nanofibers (Sánchez et al. 2016). The pulping process enriches the cellulosic fraction in the fiber, decreasing the amount of extractables, ashes, lignin and hemicellulose, as shown in Table S1. Comparatively, the α-cellulose content of wheat straw cellulosic pulp (62.0%) was similar or higher to the values presented by other cellulosic pulps from agricultural residues such as cereal straws (Espinosa et al. 2017b), corncob residue (Liu et al. 2016), banana leaves (Tarrés et al. 2017b) and date palm (Adel et al. 2018). Due to the low conditions of the pulping process, a significant part of the hemicelluloses contained in the fiber is maintained (26.1%). A high value of hemicelluloses is essential for an effective nanofibrillation process, since hemicelluloses inhibit the coalescence of cellulose fibers and contribute to the colloidal stability of the cellulose nanofibers by both electric and steric mechanism (Chaker et al. 2013; Hubbe and Rojas 2008; Iwamoto, Abe and Yano 2008). A residual lignin content in the fiber makes it possible to obtain finer cellulose nanofibers at comparable energy consumption levels (Rojo et al. 2015; Ferrer et al. 2012). This is because lignin acts as an antioxidant, preventing the union again of the previously broken covalent bonds (Solala, Iglesias and Peresin 2019). Wheat straw cellulosic pulp presents a residual lignin content of 9.0%, similar to the optimal lignin value for nanofibrillation for triticale straw (Tarrés et al. 2017a). Cellulosic pulp obtained was bleached to study the effect of lignin in the process of cellulose nanofibers isolation through different mechanical treatments (high pressure homogenizer “HPH”, ultrafine friction grinder “UFG” and twin-screw extruder “TSE”).

Once cellulose nanofibers were obtained from unbleached (LCNF) and bleached (CNF) cellulosic pulp, they were characterized in terms of nanofibrillation yield, optical transmittance, cationic demand and carboxyl content (Table 1). In general terms, the values obtained are similar to those presented in the literature for cellulose nanofibers obtained by mechanical pretreatment and treatment (Delgado-Aguilar et al. 2016; Vallejos et al. 2016; Tarrés et al. 2017a).

Several differences were observed between the different treatments, as well as depending on residual lignin content in the fiber. The process of high pressure homogenization (HPH) is the treatment that presents the best nanofibrillation yield results, which indicates that it is the most effective process for the reduction to nanometric sizes of a large portion of the original fiber, in comparison with ultrafine friction grinder (UFG) and twin-screw extruder (TSE) treatments. This fact is corroborated by the optical transmittance of

cellulose nanofiber suspension, where the highest values of this parameter coincide with the highest values of nanofibrillation yield due to the greater light scattering produced by the presence of residual fibers. These nanofibrillation yield values are comparable to those obtained by mechanical pretreatment (Vallejos et al. 2016; Delgado-Aguilar et al. 2016; Tarrés et al. 2017b; Carvalho et al. 2019), as well as enzymatic (Tarres et al. 2016; Espinosa et al. 2019b) from other raw materials. Cellulose nanofibers obtained by TEMPO-mediated oxidation shows a higher nanofibrillation yield (>90%) than the previous ones due to the greater efficiency of the cellulose oxidation that favors the separation of the nanofibers during the mechanical treatment (Chen et al. 2017; Chaker et al. 2014). Regarding the diameter, it is observed how the HPH treatment produces the nanofibers with smaller diameter (13 – 19 nm), on the other hand, the rest of the treatments also produce reduced sizes of nanofibers diameter, showing values of 22 – 30 nm for UFG and 20 – 40 nm for TSE. The nanometric diameter values were verified using AFM technique (Fig. S1). Within each treatment, significant differences in nanofibrillation performance values and diameters achieved during treatments are observed between LCNF and CNF. Greater values of nanofibrillation yield and lower diameters were achieved for LCNF due to the positive stabilizing effect of lignin during the nanofibrillation process (Rojo et al. 2015). In addition, during the bleaching process most of hemicellulose is retained in fiber, but some of them are lost together with residual lignin, decreasing its content (Solala et al. 2019), being the effectiveness of the nanofibrillation process influenced by this factor. Concerning the effect on the length of the cellulose nanofibers by the different treatments, it is observed how all the treatments produce a decrease in this parameter compared to the original value of the fiber (5522 nm). A decrease of 10.5%, 24.5% and 18.9% was produced by the HPH, UFG and TSE treatments, respectively. In addition, no significant differences in fiber shortening were observed depending on the presence of residual lignin.

The delamination process of cellulosic fiber to obtain cellulose nanofibers and the shortening produced by the different mechanical treatments was studied by means of MorFi analysis of the fiber and cellulose nanofibers (Fig. 2). MorFi analysis was used to study the morphology and number of residual fibers and fines due to it could not detect the nanosized fibers. As commented above, it is observed how the length of the fibers is shortened due to the high shear and friction forces reached in the different passes of the TSE (0p -7p), as well as in the treatments of HPH and UFG. The increase in the fines content is related to the delamination of the cellulose fiber produced, and thus to an increase in the nanofibrillation of the fiber (Rol et al. 2019c). The HPH and UFG treatments show the highest values of fine contents. In relation to the nanofibrillation yield values shown, increasing to values above 30%, starting from a value in the original fiber of around 7%, in comparison with the 24% obtained by TSE. Moreover, significant differences are found between LCNF and CNF, obtaining higher values of fine content in those fiber that contain residual lignin, as expected.

Optical microscopy images of the original fiber and the cellulose nanofiber suspension for the different treatments are displayed in Fig. 2. It is observed how the different treatments produce an increase in the fibrillation of the suspension, generating more fines

and nanofibrillated fraction. As reported previously, the HPH and UFG treatments show a higher fibrillation degree than the TSE, which presents more residual fiber due to the lower nanofibrillation yields that this treatment shows.

3.2. Effect of mechanical treatments on cellulose nanofibers quality

The cellulose nanofibers produced by the different mechanical treatments were characterized and evaluated by the quality index proposed by Desmaisons et al. (2017) obtaining the values shown in Table 2. The average size area of the residual fiber was lower for the treatments of HPH and TSE, especially for LCNF, showing a greater fiber delamination. The nanosized fraction presents value of 20 – 63%, being the HPH and TSE which presents the higher values, in agreement with the values reported by other authors for different raw materials, pretreatments and treatments (Rol et al. 2019a, Rol et al. 2019c, Rol et al. 2020, Nair et al. 2014a, Naderi et al. 2015). The presence of lignin in the fiber produces cellulose nanofibers with a twice nanosized fraction, an even higher increase than that obtained for the nanofibrillation yield. The turbidity refers to the amount of light that is dispersed by the presence of poorly fibrillated fiber, being this value closed to zero for totally nanofibrillated suspension. In this parameter, the lowest values were observed for HPH and UFG, resulting in more nanofibrillated suspensions than those obtained by TSE. Similar values was reported for enzymatic CNF treated via UFG (Desmaisons et al. 2017), and lower than others non-pretreated pulps (Rol et al. 2018). On the other hand, the CNF obtained by TEMPO-mediated oxidation, present value much lower than those presented in this work (Moser, Lindström and Henriksson 2015). The Young's modulus is directly linked to the cellulose nanofibers' interaction and aspect ratio. The lowest values of the samples obtained in this work was obtained for CNF-TSE, 12.79 GPa, being even higher than the values of CNF obtained by enzymatic (11 GPa) and cationic (9.6 GPa) pre-treated fiber. The others CNF present values of 14 GPa, similar than the values obtained for phosphorylated CNF (Rol et al. 2019a). The higher values (14 – 16 GPa) were shown by the different LCNF, similar to the obtained by others CNF reported in literature (Nair et al. 2014a).

Although the quality index (QI) was developed for the analysis of enzymatic CNF and may not be applicable to LCNF, it was used to obtain a broad view. The QI* obtained for the different samples, shows that, as well as the trend observed in the different parameters, the HPH and UFG treatments are those who presents the higher quality for cellulose nanofibers production, being 5 – 10 points higher than the values obtained by TSE. As shown in Fig. 3, there are significant differences with respect to the residual lignin content, being the QI* higher for LCNF, obtaining differences of 10 and 17 respect to CNF for HPH and UFG, respectively, and raising this difference as the number of TSE passes increase.

In order to make possible the industrial production of cellulose nanofibers, it is necessary to study the energy consumption of the different production processes. The mechanical treatments for nanofibrillation require a high energy consumption being approximately 50,000 kWh/ton for ultra-fine grinder, 30,000 kWh/ton for high pressure homogenization and 5,000 kWh/ton for twin-screw extrusion (Espinosa et al. 2019b, Chaker et al. 2014,

Spence et al. 2011). The energy consumptions of the different treatments are showed in Fig. 4. It shows that HPH and UFG requires over 30,000 kWh/ton, however, the TSE require only about 6,000 kWh/ton. It is therefore observed that for a similar quality index for the different cellulose nanofiber, their production by means of TSE treatment is convenient due to their significant energy savings. This energy consumption can be reduced by more than 30% if it is accompanied by an enzymatic or cationic pretreatment that facilitates nanofibrillation for the same quality index (Rol et al. 2019b). Despite not differences were observed between LCNF and CNF, it shows how a higher quality cellulose nanofiber is obtained for the same energy consumption by the presence of lignin in fiber (Rojo et al. 2015).

3.3. Influence of treatment and lignin content on cellulose nanofibers-based films

In order to study the effect of the production treatment and the residual lignin content on the final properties of cellulose nanofibers-based films, and to relate the quality index of the cellulose nanofibers with the final characteristics of the films, the mechanical properties, surface roughness, barrier properties and antioxidant activity were studied.

The mechanical properties of the cellulose nanofibers-based films are reported in Table 3. All the films had high Young's modulus of 13.5 – 19 GPa, high tensile strength values of 59 – 92 MPa and elongation at break values of 1.3 – 1.6%. One more time, HPH and UFG shows the better results for mechanical properties in comparison with the values obtained by TSE. A slight increase in the different mechanical properties is observed by the presence of lignin in the cellulose nanofibers. It is due to the crosslinking reaction of the lignin-related radicals that results in a densification of the cellulose nanofibers structure (Espinosa et al. 2019a, Chinga-Carrasco et al. 2012).

The effect of the treatments and lignin content on the film roughness was analyzed by laser profilometry (Fig. S2). Fig 5. shows the average values of the film surface roughness. It shows that LCNF-based films present a higher roughness than CNF-based films. Considering that the higher the nanofibrillation, the lower the roughness of the films produced, and if we consider the nanofibrillation yield and nanosized fraction values, it was to be expected that LCNF-based films present lower roughness values, however, the presence of lignin as a component within the structure of the films, results in higher surface roughness.

The barrier properties of the cellulose nanofibers-based films were analyzed in terms of water vapor permeability (WVP) and oxygen permeability (OP) and results are shows in Fig. 6. The diffusion mechanism of gases through film matrix consists of three stages: i) absorption of gas molecule in surface of the film, ii) diffusion of gas molecule through the film matrix, and iii) desorption of the gas molecule to the other side. It is observed that LCNF presents a lower OTR values in comparison with CNF. It is explained by the greater nanofibrillation of unbleached fibers that enable the production of denser and more tortuous matrices for the diffusion of gases, in addition to the compaction and filling of porous produced by lignin as an amorphous component (Nair et al. 2014b, Ferrer, Pal and Hubbe 2017). In this way, it is observed that the treatments that produce greater

nanofibrillation, such as HPH and UFG, have lower oxygen permeability values than those shown by TSE. Regarding to the WVP, it is observed that, as in the OTR, the LCNF present better water permeability values than the CNF due to the greater fibrillation and compaction of the samples. In addition, due to the initial stage of the diffusion process of the gas molecules through the films is the absorption on its surface, the water gas molecule absorption is reduced for LCNF-based films by the hydrophobic nature of the lignin (Rojo et al. 2015).

The relative antioxidant power (AOP) of the films was measured using ABTS using the ABTS assay and expressing the results in AOP per gram of film (Fig. 7). This assay is based on the measurement of the reduction of the radical (2-2' azino-di-3-ethylbenzthiazoline sulfonate) by the antioxidant compounds of the films. It is observed that there are important differences in the values of AOP for the different cellulose nanofibers, reaching values of double for LCNF (12%) in comparison with those obtained for CNF (6%). The highest AOP of LCNF is related with the antioxidant activity of the aromatic structure of lignin present in these cellulose nanofibers that act as antioxidant agent preventing or retarding the oxidation reaction produced for oxidizing agents, such as free radicals (Lu et al. 2012). On the other hand, it is not observed significant differences with respect to the AOP depending on the cellulose nanofibers production treatment.

Conclusions

Cellulose nanofibers from unbleached and bleached cellulosic pulp from wheat straw were produced by different treatments (high pressure homogenizer, ultrafine grinder and twin-screw extruder). These cellulose nanofibers were deeply characterized in order to study the effect of the nanofibrillation treatment and residual lignin content on the final properties. Different characterization parameters were used to obtain an abbreviated quality index that exposes that the presence of residual lignin in fiber allows to obtain cellulose nanofibers with a quality index value between 10 – 18 points higher, depending on the treatment used. No significant differences in energy consumption were observed in any of the treatments used based on the presence or absence of lignin in fiber. Cellulose nanofibers-based films were produced to state a relationship between films properties and cellulose nanofibers characteristics. Regarding to the film properties, the presence of lignin produces films with higher mechanical properties but greater surface roughness as demonstrated by laser profilometry. However, lignin-free nanocellulose films shows a higher oxygen transmission Rate (4 $cc/m^2/day$) and water vapor permeability (6 – 8 $g \cdot Pa^{-1} \cdot m^{-1} \cdot h^{-1} \cdot 10^{-7}$) compared with the rates obtained by lignin-containing nanocellulose (3 $cc/m^2/day$ and 4 – 7 $g \cdot Pa^{-1} \cdot m^{-1} \cdot h^{-1} \cdot 10^{-7}$). In addition, the antioxidant activity of the films produced by lignin-containing nanocellulose presents values 100% higher than bleached nanocellulose. It is concluded that the presence of lignin and ultrafine friction grinder and high pressure homogenization process produce the highest quality in cellulose nanofibers and films

Acknowledgments

The authors are grateful to Spain's DGICyT, MICINN for funding this research within the framework of the Projects CTQ2016-78729-R and supported by the Spanish Ministry of Science and Education through the National Program FPU (Grant Number FPU14/02278), and also to the staff of the Central Service for Research Support (SCAI) at the University of Córdoba.

References

Adel A, El-Shafei A, Ibrahim A, Al-Shemy M (2018) Extraction of oxidized nanocellulose from date palm (Phoenix Dactylifera L.) sheath fibers: Influence of CI and CII polymorphs on the properties of chitosan/bionanocomposite films. Ind Crop Prod 124**:**155-165.

Agate S, Joyce M, Lucia L, Pal L (2018) Cellulose and nanocellulose-based flexible-hybrid printed electronics and conductive composites – A review. Carbohyd Polym 198**:**249-260.

Besbes I, Alila S, Boufi S (2011) Nanofibrillated cellulose from TEMPO-oxidized eucalyptus fibres: Effect of the carboxyl content. Carbohyd Polym 84**:**975-983.

Boufi S, González I, Delgado-Aguilar M, Tarrés Q, Pèlach MA, Mutjé P (2016) Nanofibrillated cellulose as an additive in papermaking process: A review. Carbohyd Polym 154**:**151-166.

Campano C, Merano N, Balea A, Tarrés Q, Delgado-Aguilar M, Mutjé P, Negro C, Blanco Á (2018) Mechanical and chemical dispersion of nanocelluloses to improve their reinforcing effect on recycled paper. *Cellulose,* 25**,** 269-280.

Carvalho DMD, Moser C, Lindström ME, Sevastyanova O (2019) Impact of the chemical composition of cellulosic materials on the nanofibrillation process and nanopaper properties. Ind Crop Prod 127**:**203-211.

Chaker A, Alila S, Mutjé P, Vilar MR, Boufi S (2013) Key role of the hemicellulose content and the cell morphology on the nanofibrillation effectiveness of cellulose pulps. Cellulose: 20**-**2863-2875.

Chaker A, Mutjé P, Vilar MR, Boufi S (2014) Agriculture crop residues as a source for the production of nanofibrillated cellulose with low energy demand. Cellulose 21:4247-4259.

Chakraborty A, Sain M, Kortschot M (2005) Cellulose microfibrils: A novel method of preparation using high shear refining and cryocrushing. Holzforschung 59**:**102-107.

Chen WS, Yu HP, Liu YX, Chen P, Zhang MX, Hai YF (2011) Individualization of cellulose nanofibers from wood using high-intensity ultrasonication combined with chemical pretreatments.Carbohyd Polym 83**:**1804-1811.

Chen Y, Geng B, Ru J, Tong C, Liu H, Chen J (2017) Comparative characteristics of TEMPO-oxidized cellulose nanofibers and resulting nanopapers from bamboo, softwood, and hardwood pulps. Cellulose 24**:**4831-4844.

Chinga-Carrasco G, Kuznetsova N, Garaeva M, Leirset I, Galiullina G, Kostochko A, Syverud K (2012) Bleached and unbleached MFC nanobarriers: properties and hydrophobisation with hexamethyldisilazane. J Nanopart Res 14**:**1-10.

Chinga-Carrasco G (2013) Optical methods for the quantification of the fibrillation degree of bleached MFC materials. Micron 48**:**42-48.

Chinga-Carrasco G, Averianova N, Kondalenko O, Garaeva M, Petrov V, Leinsvang B, Karlsen T (2014). The effect of residual fibres on the micro-topography of cellulose nanopaper. Micron 56**:**80-84.

Chinga-Carrasco G (2018) Potential and Limitations of Nanocelluloses as Components in Biocomposite Inks for Three-Dimensional Bioprinting and for Biomedical Devices. Biomacromolecules 19**:**701-711.

Claramunt J, Ventura H, Toledo Filho RD, Ardanuy M (2019) Effect of nanocelluloses on the microstructure and mechanical performance of CAC cementitious matrices. Cement Concrete Rese 119**:**64-76.

de Campos A, Correa AC, Cannella D, de Teixeira E, Marconcini JM, Dufresne A, Mattoso LHC, Cassland P, Sanadi AR (2013) Obtaining nanofibers from curauá and sugarcane bagasse fibers using enzymatic hydrolysis followed by sonication. Cellulose 20**:**1491-1500.

Delgado-Aguilar M, González I, Tarrés Q, Pèlach MA, Alcalá M, Mutjé P (2016) The key role of lignin in the production of low-cost lignocellulosic nanofibres for papermaking applications. Ind Crop Prod 86**:**295-300.

Desmaisons J, Boutonnet E, Rueff M, Dufresne A, Bras J (2017) A new quarafality index for benchmarking of different cellulose nanofibrils. Carbohyd Polym 174**:**318-329.

Domenech T, Peuvrel-Disdier E, Vergnes B (2013) The importance of specific mechanical energy during twin screw extrusion of organoclay based polypropylene nanocomposites. Compos Sci Technol 75**:**7-14.

Du X, Zhang Z, Liu W, Deng Y (2017) Nanocellulose-based conductive materials and their emerging applications in energy devices - A review. Nano Energy 35**:**299-320.

Espinosa E, Tarrés Q, Delgado-Aguilar M, González I, Mutjé P, Rodríguez A (2016) Suitability of wheat straw semichemical pulp for the fabrication of lignocellulosic nanofibres and their application to papermaking slurries. Cellulose 23**:**837-852.

Espinosa E, Domínguez-Robles J, Sánchez, R, Tarrés Q, Rodríguez A (2017a) The effect of pre-treatment on the production of lignocellulosic nanofibers and their application as a reinforcing agent in paper. Cellulose 24**:**2605-2618.

Espinosa E, Sánchez R, Otero R, Domínguez-Robles J, Rodríguez A (2017b) A comparative study of the suitability of different cereal straws for lignocellulose nanofibers isolation. Int J Biol*,* 103**,** 990-999.

Espinosa E, Bascón-Villegas I, Rosal A, Pérez-Rodríguez F, Chinga-Carraco G, Rodríguez A (2019a) PVA/(ligno)nanocellulose biocomposite films. Effect of residual lignin content on structural, mechanical, barrier and antioxidant properties. Int J Biol Macromol 141**:**197-206.

Espinosa E, Rol F, Bras J, Rodríguez A (2019b) Production of lignocellulose nanofibers from wheat straw by different fibrillation methods. Comparison of its viability in cardboard recycling process. J Cean Prod 239**:**118083.

Fall AB, Lindström SB, Sundman O, Ödberg L, Wågberg L (2011) Colloidal Stability of Aqueous Nanofibrillated Cellulose Dispersions. Langmuir 27**:**11332-11338.

Ferrer A, Pal L, Hubbe M (2017) Nanocellulose in packaging: Advances in barrier layer technologies. Ind Crop Prod 95:574-582.

Ferrer A, Quintana E, Filpponen I, Solala I, Vidal T, Rodríguez A, Laine J, Rojas OJ (2012) Effect of residual lignin and heteropolysaccharides in nanofibrillar cellulose and nanopaper from wood fibers. Cellulose 19**:**2179-2193.

Fillat Ú, Wicklein B, Martín-Sampledro R, Ibarra D, Ruiz-Hitzky E, Valencia C, Sarrión A, Castro E, Eugenio ME (2018) Assessing cellulose nanofiber production from olive tree pruning residue. Carbohyd Polym 179**:**252-261.

García A, González Alriols M, Spigno G, Labidi J (2012) Lignin as natural radical scavenger. Effect of the obtaining and purification processes on the antioxidant behaviour of lignin. Biochem Eng J 67**:**173-185.

Gogoi BK, Oswalt AJ, Choudhury GS (1996) Reverse screw element(s) and feed Composition effects during twin-screw extrusion of rice flour and fish muscle blends. J Food Sci 61:590-595.

Hubbe MA, Rojas OJ (2008) Colloidal stability and aggregation of lignocellulosic materials in aqueous suspension: a review. BioResources 3(4).

Iwamoto S, Abe K, Yano H (2008) The effect of hemicelluloses on wood pulp nanofibrillation and nanofiber network characteristics. Biomacromolecules 9:1022-1026.

Karkhanis SS, Stark NM, Sabo RC, Matuana LM (2018) Water vapor and oxygen barrier properties of extrusion-blown poly(lactic acid)/cellulose nanocrystals nanocomposite films. Compos Part A-Appl S 114:204-211.

Kumode MMN, Bolzon GIM, Magaelhães WLE, Kestur SG (2017) Microfibrillated nanocellulose from balsa tree as potential reinforcement in the preparation of 'green' composites with castor seed cake. J Clean Prod 149:1157-1163.

Li JH, Wei XY, Wang QH, Chen JC, Chang G, Kong LX, Su JB, Liu YH (2012) Homogeneous isolation of nanocellulose from sugarcane bagasse by high pressure homogenization. Carbohyd Polym 90:1609-1613.

Liang M, Huff HE, Hsieh FH (2002) Evaluating energy consumption and efficiency of a twin-screw extruder. J Food Sci 67:1803-1807.

Liu C, Li B, Du H, Lv D, Zhang Y, Yu G, Mu X, Peng H (2016) Properties of nanocellulose isolated from corncob residue using sulfuric acid, formic acid, oxidative and mechanical methods. Carbohyd Polym 151:716-724.

Lu Q, Liu W, Yang L, Zu Y, Zu B, Zhu M, Zhang Y, Zhang X, Zhang R, Sun Z, Huang J, Zhang X, Li W (2012) Investigation of the effects of different organosolv pulping methods on antioxidant capacity and extraction efficiency of lignin. Food Chem 131:313-317.

Marx-Figini M (1987) The acid-catalyzed degradation of cellulose linters in distinct ranges of degree of polymerization. J Appl Polym Sci 33:2097-2105.

Morais JPS, Rosa MDF, de Souza Filho MDSM, Nascimento LD, do Nascimento DM, Cassales AR (2013) Extraction and characterization of nanocellulose structures from raw cotton linter. Carbohyd Polym 91:229-235.

Moser C, Lindström ME, Henriksson G (2015) Toward Industrially Feasible Methods for Following the Process of Manufacturing Cellulose Nanofibers. BioResources 10:2

Naderi A, Lindström T, Sundström J (2015) Repeated homogenization, a route for decreasing the energy consumption in the manufacturing process of carboxymethylated nanofibrillated cellulose? Cellulose 22:1147-1157.

Nair SS, Zhu JY, Deng Y, Ragauskas AJ (2014a) Characterization of cellulose nanofibrillation by micro grinding. J Nanopart Res 16:2349

Nair SS, Zhu JY, Deng Y, Ragasuskas AJ (2014b) High performance green barriers based on nanocellulose. Sustain Chem Process 2:23

Pääkkö M, Ankefors M, Kosonen H, Nykänen A, Ahola S, Österberg M, Ruokolainen J, Laine J, Larsson PT, Ikkala O, Lindström T (2007) Enzymatic Hydrolysis Combined with Mechanical Shearing and High-Pressure Homogenization for Nanoscale Cellulose Fibrils and Strong Gels. Biomacromolecules 8:1934-1941.

Rambabu N, Panthapulakkal S, Sain M, Dalai AK (2016) Production of nanocellulose fibers from pinecone biomass: Evaluation and optimization of chemical and mechanical treatment conditions on mechanical properties of nanocellulose films. Ind Crop Prod 83:746-754.

Rojo E, Peresin MS, Sampson WW, Hoeger IC, Vartiainen J, Laine J, Rojas OJ (2015) Comprehensive elucidation of the effect of residual lignin on the physical, barrier, mechanical and surface properties of nanocellulose films. Green Chem 17:1853-1866.

Rol F, Karakashov B, Nechyporchuk O, Terrien M, Meyer V, Dufresne A, Belgacem MN, Bras J (2017) Pilot-Scale Twin Screw Extrusion and Chemical Pretreatment as an Energy-Efficient Method for the Production of Nanofibrillated Cellulose at High Solid Content. ACS Sustain Chem Eng 5:6524-6531

Rol F, Banvillet G, Meyer V, Petit-Conil M, Bras J (2018) Combination of twin-screw extruder and homogenizer to produce high-quality nanofibrillated cellulose with low energy consumption. J Mater Sci 53:12604-12615.

Rol F, Belgacem N, Meyer V, Petit-Conil M, Bras J (2019a) Production of fire-retardant phosphorylated cellulose fibrils by twin-screw extrusion with low energy consumption. Cellulose 26:5635-5651.

Rol F, Saini S, Meyer V, Petit-Conil M, Bras J (2019b) Production of cationic nanofibrils of cellulose by twin-screw extrusion. Ind Crop Prod 137:81-88.

Rol F, Vergnes B, El Kissi N, Bras J (2019c) Nanocellulose Production by Twin-Screw Extrusion: Simulation of the Screw Profile To Increase the Productivity. ACS Sustain Chem Eng (In press).

Rol F, Sillard C, Bardet M, Yarava JR, Emsley L, Gablin C, Léonard D, Belgacem N, Bras J (2020) Cellulose phosphorylation comparison and analysis of phosphorate position on cellulose fibers. Carbohyd Polym 229:115294.

Ruiz-Palomero C, Laura Soriano M, Valcárcel M (2017) Detection of nanocellulose in commercial products and its size characterization using asymmetric flow field-flow fractionation. Microchim Acta 184:1069-1076.

Saito T, Kimura S, Nishiyama Y, Isogai A (2007) Cellulose Nanofibers Prepared by TEMPO-Mediated Oxidation of Native Cellulose. Biomacromolecules 8:2485-2491.

Sánchez R, Espinosa E, Domínguez-Robles J, Loaiza JM, Rodríguez A (2016) Isolation and characterization of lignocellulose nanofibers from different wheat straw pulps. Int J Biol Macromol 92:1025-1033.

Shinoda R, Saito T, Okita Y, Isogai A (2012) Relationship between Length and Degree of Polymerization of TEMPO-Oxidized Cellulose Nanofibrils. Biomacromolecules 13:842-849.

Siqueira G, Tapin-Lingua S, Bras J, da Silva Pere, Dufresne A (2010) Morphological investigation of nanoparticles obtained from combined mechanical shearing, and enzymatic and acid hydrolysis of sisal fibers. Cellulose 17:1147-1158.

Solala I, Iglesias MC, Peresin MS (2019) On the potential of lignin-containing cellulose nanofibrils (LCNFs): a review on properties and applications. Celluose (In press)

Spence KL, Venditti RA, Rojas OJ, Habibi Y, Pawlak JJ (2011) A comparative study of energy consumption and physical properties of microfibrillated cellulose produced by different processing methods. Cellulose 18:1097-1111.

Tarres Q, Saguer E, Pèlach MA, Alcalá M, Delgado-Aguilar M, Mutjé P (2016) The feasibility of incorporating cellulose micro/nanofibers in papermaking processes: the relevance of enzymatic hydrolysis. Cellulose 23:1433-1445.

Tarrés Q, Ehman NV, Vallejos ME, Area MC, Delgado-Aguilar M, Mutjé P (2017a) Lignocellulosic nanofibers from triticale straw: The influence of hemicelluloses and lignin in their production and properties. Carbohyd Polym 163:20-27.

Tarrés Q, Espinosa E, Domínguez-Robles J, Rodríguez A, Mutjé P, Delgado-Aguilar M (2017b) The suitability of banana leaf residue as raw material for the production of high lignin content micro/nano fibers: From residue to value-added products. Ind Crop Prod 99:27-33.

Torstensen JØ, Helberg RML, Deng L, Gregersen ØW, Syverud K (2019) PVA/nanocellulose nanocomposite membranes for CO2 separation from flue gas. Int J Greenh Gas Con 81:93-102.

Vallejos ME, Felissia FE, Area MC, Ehman NV, Tarrés Q, Mutjé P (2016) Nanofibrillated cellulose (CNF) from eucalyptus sawdust as a dry strength agent of unrefined eucalyptus handsheets. Carbohyd Polym 139**:**99-105.

Wang Q, Yao Q, Liu J, Sun J, Zhu Q, Chen H (2019) Processing nanocellulose to bulk materials: a review. Cellulose 26**:**7585-7617.

Wang W, Mozuch MD, Sabo RC, Kersten P, Zhu Jy, Jin Y (2015) Production of cellulose nanofibrils from bleached eucalyptus fibers by hyperthermostable endoglucanase treatment and subsequent microfluidization. Cellulose 22**:**351-361.

Yousefi H, Faezipour M, Nishin T, Shakeri A, Ebrahimi G (2011) All-cellulose composite and nanocomposite made from partially dissolved micro- and nanofibers of canola straw. Polym J 43**:**559-564.

Figure Captions

Fig. 1. Morphological analysis of the different cellulose nanofibers

Fig. 2. Optical microscopy images for: a) Bleached initial fiber, b) CNF-TSE, c) CNF-HPH, d) CNF-UFG, e) Unbleached initial fiber, f) LCNF-TSE, g) LCNF-HPH and h) LCNF-UFG

Fig. 3. Abbreviated quality index (QI*) differences between unbleached and bleached cellulose nanofibers

Fig. 4. Energy consumption of the different nanofibrillation treatments

Fig. 5. Surface roughness of the cellulose nanofibers-based films

Fig. 6. Comparison of the unbleached (black) and bleached (grey) cellulose nanofibers-based films barrier properties respect to the nanofibrillation treatment

Fig. 7. Comparison of the unbleached (black) and bleached (grey) cellulose nanofibers-based films antioxidant activity respect to the nanofibrillation treatment

Use of multi-factorial analysis to determine the quality of cellulose nanofibers. Effect of nanofibrillation treatment and residual lignin content

Eduardo Espinosa[a], Fleur Rol[b], Alejandro Rodríguez[a], Julien Bras[bc]

[a] Universidad de Córdoba, Departamento de Ingeniería Química, Campus de Rabanales, 14014 Córdoba, Spain

[b] Univ. Grenoble Alpes, CNRS, Grenoble INP, LGP2, F-38000 Grenoble, France

[c] Institut Universitaire de France (IUF), F-75000 Paris, France

* Corresponding author: eduardo.espinosa@uco.es

Cellulose

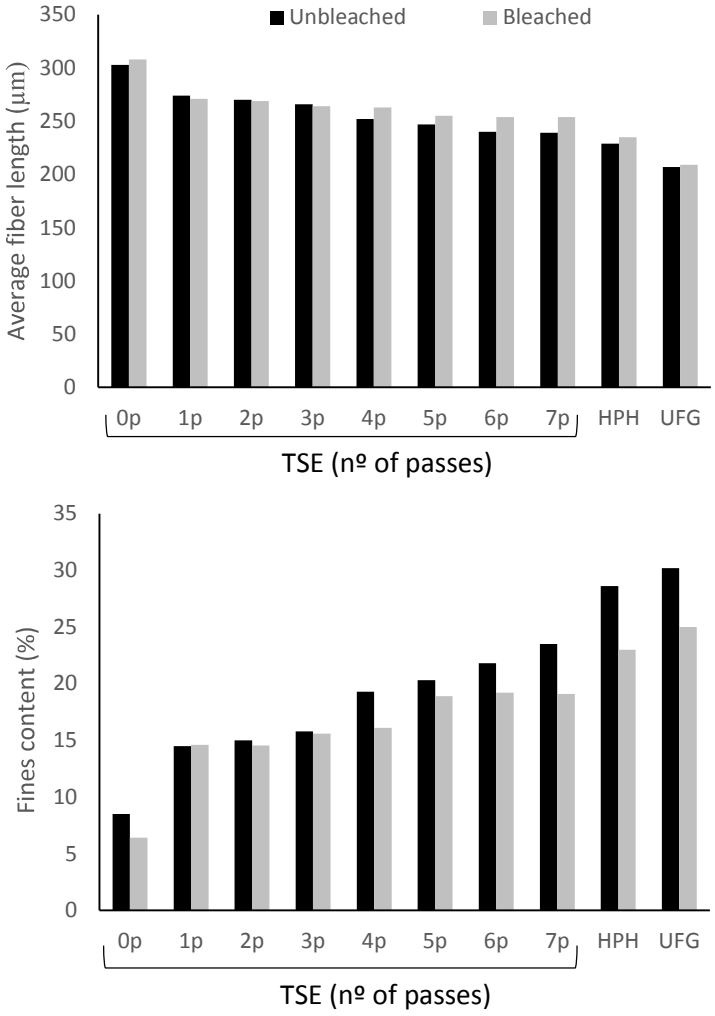

Fig. 1. Morphological analysis of the different cellulose nanofibers

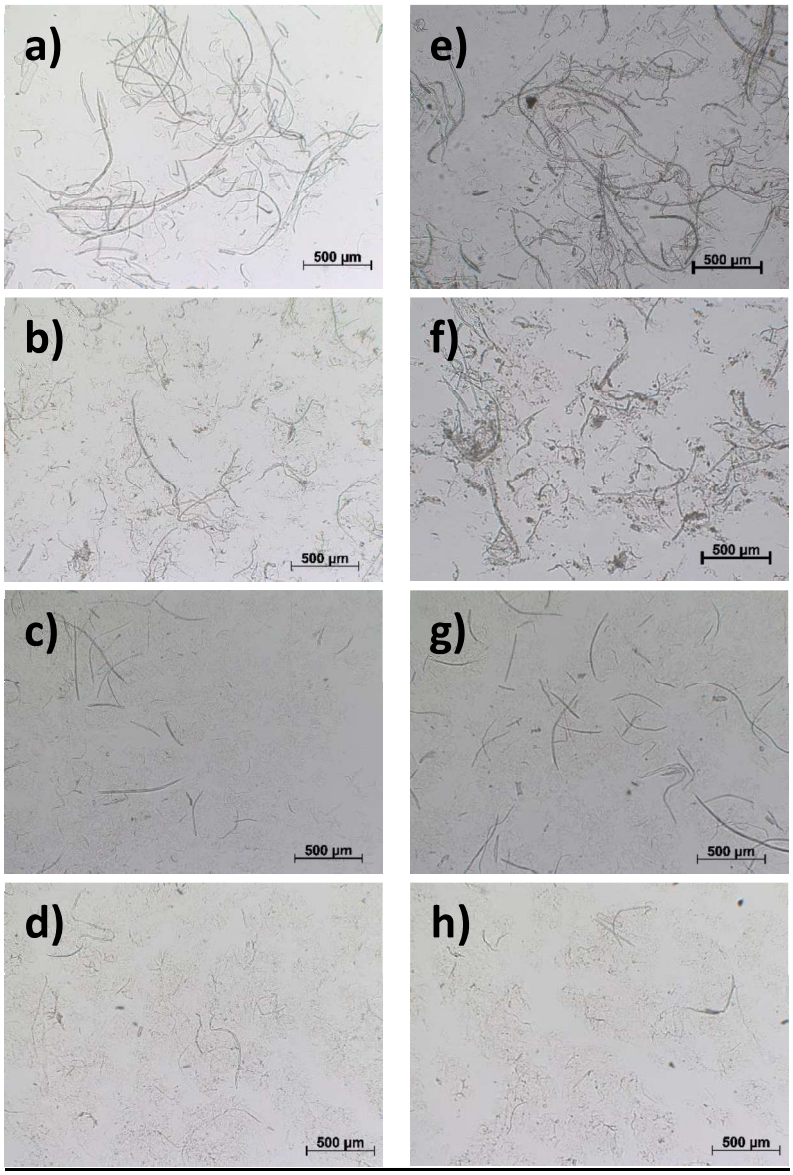

Fig. 2. Optical microscopy images for: a) Bleached initial fiber, b) CNF-TSE, c) CNF-HPH, d) CNF-UFG, e) Unbleached initial fiber, f) LCNF-TSE, g) LCNF-HPH and h) LCNF-UFG.

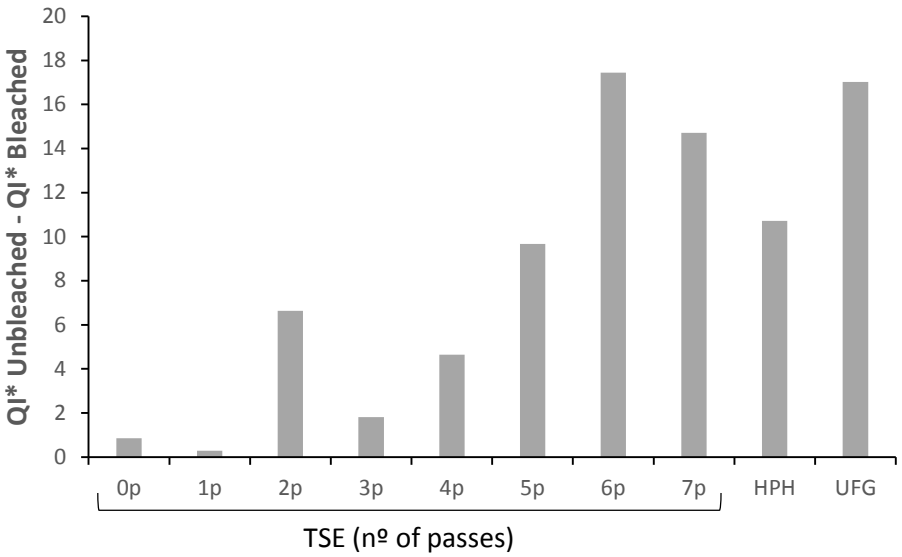

Fig. 3. Abbreviated quality index (QI*) differences between unbleached and bleached cellulose nanofibers

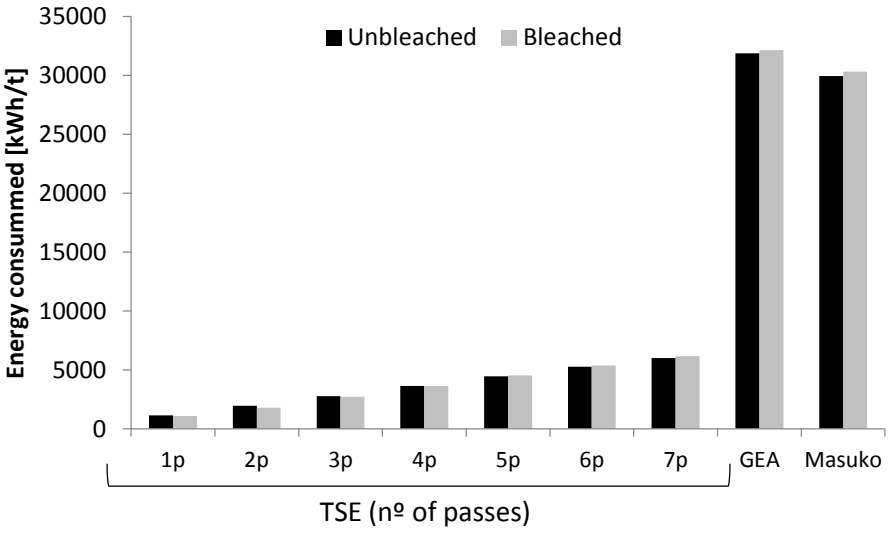

Fig. 4. Energy consumption of the different nanofibrillation treatments.

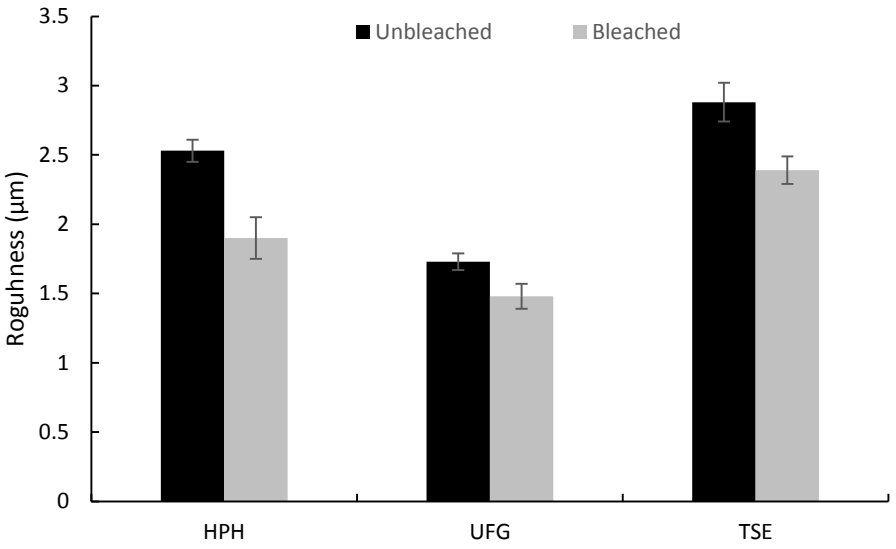

Fig. 5. Surface roughness of the cellulose nanofibers-based films

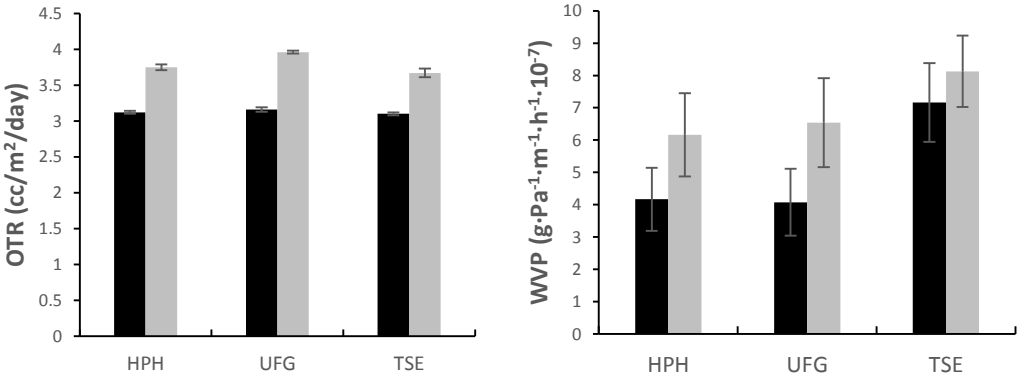

Fig. 6. Comparison of the unbleached (black) and bleached (grey) cellulose nanofibers-based films barrier properties respect to the nanofibrillation treatment

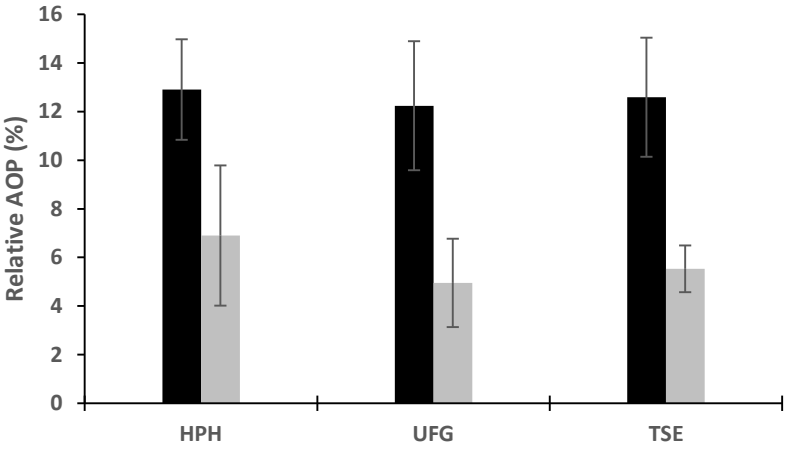

Fig. 7. Comparison of the unbleached (black) and bleached (grey) cellulose nanofibers-based films antioxidant activity respect to the nanofibrillation treatment

Use of multi-factorial analysis to determine the quality of cellulose nanofibers. Effect of nanofibrillation treatment and residual lignin content

Eduardo Espinosa[a], Fleur Rol[b], Alejandro Rodríguez[a], Julien Bras[bc]

[a] Universidad de Córdoba, Departamento de Ingeniería Química, Campus de Rabanales, 14014 Córdoba, Spain

[b] Univ. Grenoble Alpes, CNRS, Grenoble INP, LGP2, F-38000 Grenoble, France

[c] Institut Universitaire de France (IUF), F-75000 Paris, France

* Corresponding author: eduardo.espinosa@uco.es

Cellulose

Table 1. Cellulose nanofibers characterization

Sample	η (%)	T_{800} (%)	CD (μeq·g/g)	CC (μeq·g/g)	$\sigma_{surface}$ (m^2/g)	D (nm)	L (mm)	Aspect ratio
CNF-HPH	27.09±5.26	34	328.69±37.19	51.24±1.19	134.0	19	4943	247
LCNF-HPH	55.60±5.26	55	441.06±7.50	64.41±2.36	183.4	13	4939	379
CNF-UFG	21.39±2.03	18	215.05±9.01	42.80±12.97	83.9	30	4169	139
LCNF-UFG	35.80±1.20	25	269.19±38.07	41.05±7.04	111.1	22	4163	189
CNF-TSE	12.11±0.47	14	149.66±38.48	33.59±1.19	56.5	44	4476	102
LCNF-TSE	15.17±4.20	16	307.83±9.68	49.35±1.73	125.8	20	4437	221

η: Nanofibrillation yield; T: Optical transmittance at 800 nm; CD: Cationic demand; CC: Carboxyl content; $\sigma_{surface}$: Specific surface area; D: Diameter; L: Length

Table 2. Quality indexes of cellulose nanofiber produced by different treatments

Sample	Average size (μm^2)	Nanosized fraction (%)	Turbidity (NTU)	Young's modulus (GPa)	Quality Index
LCNF-HPH	26.98 ± 6.63	60.93 ± 1.32	205.66 ± 5.86	16.87 ± 0.89	74.94 ± 1.07
CNF-HPH	37.59 ± 10.36	32.19 ± 2.57	433.00 ± 18.91	14.50 ± 1.10	64.22 ± 1.23
LCNF-UFG	19.39 ± 2.49	62.48 ± 0.20	245.17 ± 6.33	16.65 ± 0.71	76.49 ± 1.07
CNF-UFG	46.14 ± 7.30	36.51 ± 8.01	274.00 ± 6.72	14.50 ± 0.90	59.47 ± 5.45
LCNF-TSE	34.18 ± 2.77	60.96 ± 8.99	365.00 ± 8.48	14.20 ± 0.87	69.60 ± 4.30
CNF-TSE	59.90 ± 10.24	20.37 ± 5.19	239.13 ± 8.32	12.79 ± 0.60	54.88 ± 0.66

Table 3. Mechanical properties of the cellulose nanofibers-based films

Sample	Tensile strength (MPa)	Elongation at break (%)	Young's modulus (GPa)
LCNF-HPH	91.45 ± 10.77	1.59 ± 0.40	17.55 ± 0.17
CNF-HPH	76.57 ± 6.21	1.34 ± 0.40	16.91 ± 0.31
LCNF-UFG	84.03 ± 12.11	1.49 ± 0.52	18.99 ± 0.36
CNF-UFG	76.57 ± 6.21	1.34 ± 0.40	14.52 ± 0.31
LCNF-TSE	70.83 ± 4.36	1.59 ± 0.52	14.02 ± 0.27
CNF-TSE	59.41 ± 2.30	1.30 ± 0.22	13.53 ± 0.22

Cover Letter

Click here to access/download

Supplementary Material

Supplementary Data.docx